Vitamin D is an endogenous partial agonist of the transient receptor potential vanilloid 1 channel

Wentong Long[1,2] , Mohammad Fatehi[1,2], Shubham Soni[1] , Rashmi Panigrahi[3], Koenraad Philippaert[1,2,4] , Yi Yu[1,2], Rees Kelly[5], Brett Boonen[4] , Amy Barr[1,2], Dominic Golec[1,2], Scott A. Campbell[1,2] , Katarina Ondrusova[1,2], Matt Hubert[1,2], Troy Baldwin[5], M. Joanne Lemieux[3] and Peter E. Light[1,2]

[1]*Alberta Diabetes Institute, Faculty of Medicine & Dentistry, University of Alberta, Edmonton, Canada*
[2]*Departments of Pharmacology, Faculty of Medicine & Dentistry, University of Alberta, Edmonton, Canada*
[3]*Biochemistry, Faculty of Medicine & Dentistry, University of Alberta, Edmonton, Canada*
[4]*Laboratory for Ion Channel Research, Department of Cellular and Molecular Medicine, VIB Center for Brain and Disease Research, KU Leuven, Leuven, Belgium*
[5]*Medical Microbiology & Immunology, Faculty of Medicine & Dentistry, University of Alberta, Edmonton, Canada*

Edited by: Peying Fong & Reinhold Penner

The Journal of Physiology

Key points

- 25-Hydroxyvitamin D (25OHD) is a partial agonist of TRPV1 whereby 25OHD can weakly activate TRPV1 yet antagonize the stimulatory effects of the full TRPV1 agonists capsaicin and oleoyl dopamine.
- 25OHD binds to TRPV1 within the same vanilloid binding pocket as capsaicin.
- 25OHD inhibits the potentiating effects of PKC-mediated TRPV1 activity.
- 25OHD reduces T-cell activation and trigeminal neuron calcium signalling mediated by TRPV1 activity.
- These results provide evidence that TRPV1 is a novel receptor for the biological actions of vitamin D in addition to the well-documented effects of vitamin D upon the nuclear vitamin D receptor.
- The results may have important implications for our current understanding of certain diseases where TRPV1 and vitamin D deficiency have been implicated, such as chronic pain and autoimmune diseases, such as type 1 diabetes.

Abstract The capsaicin receptor TRPV1 plays an important role in nociception, inflammation and immunity and its activity is regulated by exogenous and endogenous lipophilic ligands. As vitamin D is lipophilic and involved in similar biological processes as TRPV1, we hypothesized that

Wentong Long obtained her BSc and PhD in Physiology at the University of Alberta. She is a trained electrophysiologist and molecular biologist, and she has worked on numerous projects that have focused on protein structure–function studies on glucose transporters, TRP channels and sodium channels. This current project has expanded her research skills in *ex vivo* primary cell calcium imaging and flow cytometry studies on primary mouse T-cells and trigeminal neurons. She is keen to pursue a research career with a focus on precision medicine. **Peter E. Light's** research laboratory is located in the Alberta Diabetes Institute, Department of Pharmacology and the Faculty of Medicine and Dentistry at the University of Alberta. His lab researches ion transport processes controlling cellular excitability, utilizing a combination of electrophysiological, live-cell imaging, biochemical and molecular techniques to study the biophysics, physiology and pharmacology of ion channels and exchangers at the molecular, cellular, organ and whole organism levels.
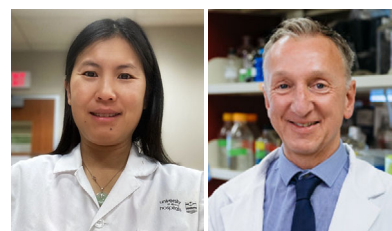
it directly regulates TRPV1 activity and function. Our calcium imaging and electrophysiological data demonstrate that vitamin D (25-hydroxyvitamin D (25OHD) and 1,25-hydroxyvitamin D (1,25OHD)) can weakly activate TRPV1 at physiologically relevant concentrations (100 nM). Furthermore, both 25OHD and 1,25OHD can inhibit capsaicin-induced TRPV1 activity (IC_{50} = 34.3 ± 0.2 and 11.5 ± 0.9 nM, respectively), but not pH-induced TRPV1 activity, suggesting that vitamin D interacts with TRPV1 in the same region as the TRPV1 agonist capsaicin. This hypothesis is supported by our *in silico* TRPV1 structural modelling studies, which place 25OHD in the same binding region as capsaicin. 25OHD also attenuates PKC-dependent TRPV1 potentiation via interactions with a known PKC phospho-acceptor residue in TRPV1. To provide evidence for a physiological role for the interaction of vitamin D with TRPV1, we employed two different cellular models known to express TRPV1: mouse CD4^{+} T-cells and trigeminal neurons. Our results indicate that 25OHD reduces TRPV1-induced cytokine release from T-cells and capsaicin-induced calcium activity in trigeminal neurons. In summary, we provide evidence that vitamin D is a novel endogenous regulator of TRPV1 channel activity that may play an important physiological role in addition to its known effects through the canonical nuclear vitamin D receptor pathway.

Introduction

The transient receptor potential (TRP) family of cation channels are expressed in many tissues throughout the body where they act as sensors of thermal, chemical and mechanical signals that contribute to the sensory transduction of environmental stimuli such as temperature, taste and nociception (Benham *et al.* 2003; Julius, 2013; Altier, 2015). TRP channels are also intimately involved in metabolic, inflammatory and immune system regulation (Lee & Gu, 2009; Gram *et al.* 2017; Christie *et al.* 2018). Therefore, TRP channels have attracted significant pharmaceutical interest (Carnevale & Rohacs, 2016; Moran, 2018).

The TRP vanilloid subfamily member 1 (TRPV1) channel was the first mammalian TRP channel to be discovered (Caterina *et al.* 1997) and is the most widely characterized. TRPV1 is also known as the capsaicin receptor as it is the molecular target for the potent agonist capsaicin found in hot chili peppers (Caterina *et al.* 1997; Elokely *et al.* 2016). TRPV1 activity can also be regulated by endogenous agonists such as anandamide (Ross, 2003) and *N*-oleoyldopamine (OLDA) (Chu *et al.* 2003; Zhong & Wang, 2008), phosphoinositides (Prescott & Julius, 2003; Lukacs *et al.* 2007), long chain acyl CoA esters (Prescott & Julius, 2003; Yu *et al.* 2014) and oxytocin (Nersesyan *et al.* 2017). TRPV1 activity is also modulated by phosphorylation; for example, protein kinase C is a key regulator of TRPV1 sensitivity to activation and desensitization by known stimuli (Bhave *et al.* 2003; Mandadi *et al.* 2004; Studer & McNaughton, 2010). With respect to the immune system, TRPV1 activity is thought to play an important role in regulating immune cell activation and cytokine production through the control of intracellular calcium (Bertin *et al.* 2014; Omari *et al.* 2017). Moreover, TRPV1 may also be involved in auto-immune diseases such as type 1 diabetes (T1D) (Tsui *et al.* 2007) and multiple sclerosis (Bassi *et al.* 2019).

A number of endogenous ligands for TRPV1 have previously been identified suggesting that additional ligands with differing roles and properties likely exist. One potential candidate is vitamin D, as its deficiency (Holick, 2007) is similarly associated with metabolic disorders (Grammatiki *et al.* 2017; Li *et al.* 2018), nociceptive disorders (Yong *et al.* 2017), inflammation and auto-immune diseases such as T1D (Altieri *et al.* 2017), multiple sclerosis (McLaughlin *et al.* 2018; Berezowska *et al.* 2019) and psoriasis (Barrea *et al.* 2017). Taken together, these findings suggest there may be a common convergent mechanism in these diseases in which both TRPV1 and vitamin D are involved.

Vitamin D is a lipophilic secosteroid that is first synthesized in the skin as cholecalciferol after exposure to sunlight. Cholecalciferol is then metabolized in the liver and kidney to form calcifediol (25-hydroxyvitamin D; 25OHD) and calcitriol (1,25-hydroxyvitamin D; 1,25OHD), respectively. As 25OHD is the major circulating form of vitamin D, and its levels are used clinically to estimate optimum vitamin D levels in the blood, which are considered to be ∼80 nmol or higher (Hollis, 2005; Holick, 2007). In contrast, 1,25OHD exhibits activity against the nuclear vitamin D receptor (VDR) in the picomolar range, with a short half-life in the blood. The canonical physiological mechanism of action of vitamin D is thought to involve 1,25OHD binding to the VDR, resulting in

alterations in gene transcription (Kato, 2000; Pike & Meyer, 2010). With respect to the immune system, studies have shown that 1,25OHD can reduce inflammatory cytokine production from T-cells (Von Essen *et al.* 2010; Cantorna *et al.* 2015). However, the precise mechanism remains to be elucidated, considering that the VDR is not expressed in naïve T-cells (Von Essen *et al.* 2010). Therefore, 25OHD and 1,25OHD may be acting on additional as yet undiscovered pathways to regulate cellular function in a variety of tissues. Like 25OHD and 1,25OHD, known exogenous and endogenous TRPV1 ligands are predominately lipophilic. Therefore, as TRPV1 and vitamin D display a substantial overlap in the disease profiles in which they are both involved, we hypothesized that 25OHD and 1,25OHD may be endogenous ligands for TRPV1.

Herein, we detail our discovery that vitamin D is a partial agonist of TRPV1 at physiologically relevant circulating nanomolar concentrations (Hollis, 2005; Holick, 2007). Through molecular docking simulations and site-directed mutagenesis, we determined that 25OHD binds to the same region of TRPV1 as the known TRPV1 agonist capsaicin. *In vitro* models of T-cell activation and nociception demonstrate that 25OHD and 1,25OHD also alter TRPV1-mediated cellular function. We conclude that 25OHD and 1,25OHD are novel endogenous TRPV1 partial agonists that may regulate a variety of cellular functions in which TRPV1 is involved via a mechanism independent of the VDR.

Methods

Cell culture, protein expression, mutagenesis and experimental reagents

Human embryonic kidney 293T (HEK293T) cells were cultured in Dulbecco's modified Eagle's medium (DMEM) (unless specified, all media and chemicals were purchased from Sigma-Aldrich, St Louis, MO, USA) supplemented with 7.5% fetal bovine serum and 1% penicillin/streptomycin) at 37°C in an incubator with 5% CO_2. The human TRPV1 gene in pCMV6 vector (OriGene, Rockville, MD, USA, cat. no. SC128105 USA) was co-transfected with a green fluorescent protein (GFP) or mCherry vector into HEK293T cells for visual identification of transfected cells. Point mutations were introduced into TRPV1 by site-directed mutagenesis (QuikChange, part number: 200 521, Agilent Technologies, Santa Clara, CA, USA). The sequence of the primers used are listed in Table 1. Unless otherwise stated, experimental reagents were dissolved in dimethylsulfoxide (DMSO) as stock solutions and added to the experimental solutions immediately prior to use to obtain the desired final concentration (<0.001% DMSO).

CD4$^+$ T-cell isolation and purification

C57BL/6 mice were obtained from Charles River and housed under a 12:12 light–dark cycle with free access to food and water. All animal experiments were carried out in accordance with institutional guidelines and were approved by the animal ethics committee of the University of Alberta. Mouse lymphocytes were isolated from C57BL/6 mice and T-cell enrichment via negative selection was performed (EasySep^{TM} Stemcell Technologies, Vancouver, Canada) using a fluorescein isothiocyanate-conjugated anti-CD45R antibody (BD Bioscience, San Jose, CA, USA). Enriched T-cells were cultured at 37°C in 24-well plates (5×10^6 cells/well) in 500 µL RPMI medium with 10% fetal bovine serum, 5% serum complex and 1% penicillin/streptomycin. Anti-CD3 and anti-CD28 antibodies (BD Bioscience) were used to activate the T-cells for 24 h; 100 nM 25OHD, 1,25OHD or 5 µM capsazepine was added to the culture medium at the start of activation. After 24 h, the cells underwent flow cytometry analysis for the detection of tumour necrosis factor α (TNFα) and interferon γ (INFγ) to assess T-cell activation.

Ca^{2+} imaging of recombinant human TRPV1

HEK293T were co-transfected with expression vectors encoding TRPV1 and mCherry for 16–18 h and mCherry fluorescence was used to confirm transfection. After 24 h, the cells were trypsinized and plated onto poly-L-lysine-coated coverslips and incubated at 37°C for 3 h. Prior to imaging, cells were incubated in DMEM containing 2 µM Fluo-5F-AM (AAT Bioquest, Sunnyvale, CA, USA, cat. no. 20560) for 30 min at 37°C, after which they were transferred to a 1 ml imaging chamber containing a superfusion buffer (in mM: 155 NaCl, 5 KCl, 2 CaCl$_2$, 1 MgCl$_2$, 5 Hepes and 10 glucose, pH 7.4). A gravity-driven multichannel superfusion system ($\sim$2 ml min^{-1}) was used to perfuse cells with experimental solutions. All experiments were performed at room temperature. An Olympus IX83 microscope and a Hamamatsu Orca-Flash 4.0 (Hamamatsu, Bridgewater NJ, USA) was used to capture images. Transfected cells were identified by mCherry fluorescence (560 nm excitation, 610 emission). For calcium imaging using Fluo-5, cells were excited at 488 nm for 200 ms at 0.3 Hz and the emitted fluorescence images captured at 520 nm. All experiments were performed at room temperature.

Electrophysiology

For the measurement of whole-cell TRPV1 currents, transfected cells were superfused with bath solution containing (in mM): 140 NaCl, 5 KCl, 1 MgCl$_2$, 2 CaCl$_2$, 10 glucose,

Table 1. Primer sets for single amino acid mutagenesis of TRPV1

Mutagenesis site	Primers	
S502A	Forward	CAGAGGCGGCCGGCGATGAAG
	Reverse	CTTCATCGCCGGCCGCCTCTG
Y511A	Forward	CCTGTTTGTGGACAGCGACAGTGAGATGCTTTTC
	Reverse	GAAAAGCATCTCACTGTCGCTGTCCACAAACAGG
S512A	Forward	GTTTGTGGACAGCTACGCTGAGATGC
	Reverse	GCATCTCAGCGTAGCTGTCCACAAAC
T550A	Forward	CTGGCCTTGGGCTGGGACAACATGCTCTACTAC
	Reverse	GTAGTAGAGCATGTTGTCCCAGCCCAAGGCCAG
L553A	Forward	GACCAACATGGCCTACTACAC
	Reverse	GTGTAGTAGGCCATGTTGGTC
E570A	Forward	CGTCATGATAGCGAAGATGATCC
	Reverse	GGATCATCTTCGCTATCATGACG
T704A	Forward	CAGAGAGCCATCGCCATCCTGGACACGG
	Reverse	CCGTGTCCAGGATGGCGATGGCTCTCTG
S801A	Forward	GAGAGGCAGCTGCTCGAGATAGGCAGTCTGC
	Reverse	GCAGACTGCCTATCTCGAGCAGCTGCCTCTC

10 Hepes (pH 7.4). The pipette solution contained (in mM): 130 CsCl, 2 NaCl, 1 MgCl$_2$, 10 Hepes (pH 7.4). For cell-attached single TRPV1 channel current recording, cells were superfused with bath solution containing (in mM): 140 potassium gluconate, 2.5 KCl, 1 MgCl$_2$, 2 CaCl$_2$, 10 glucose, 10 Hepes (pH 7.4). The pipette solution contained (in mM): 140 sodium gluconate, 10 NaCl, 1 MgCl$_2$, 1.5 EGTA, 10 Hepes (pH 7.4 with NaOH). After giga-seal formation, for the cell-attached single channel recordings the patch was held at −60 mV. For whole-cell current recordings, after patch rupture the cells were held at −60 mV. All recordings were performed using an Axopatch 200B patch-clamp amplifier using Clampex 9.2 and Clampfit 9.2 software (Molecular Devices, San Jose, CA, USA) for data acquisition and analysis. Channel open dwell time and opening events per second were presented as total absolute number of all the events collected. Channel open probabilities were presented as fold changes normalized to the control values. All grouped data are presented as means ± standard deviation.

In silico modelling and docking of 25OHD to human TRPV1

The human TRPV1 sequence (Q8NER1, 839 residues per monomer) was downloaded from UniProtKB/Swiss-Prot (www.uniprot.org). A homology modelling approach was utilized to prepare the 3D structure of human TRPV1 using the cryoEM structure of rat TRPV1 as the template (Liao *et al.* 2013). The ITASSER suite was used for modelling (Yang & Zhang, 2015). The 3D structures of capsaicin, capsazepine and 25OHD were obtained from PubChem. The PDB files of the above ligands and the human TRPV1 receptor were then prepared for AutoDock Vina docking (Trott & Olson, 2010). Hydrogen and partial charges were added, followed by 10,000 minimization steps and the modified coordinates were saved in pdbqt format. A grid was made either by taking the reference ligand or by selecting the active site residues involved in the binding of the substrate. Flexible ligand docking was carried out using the standard precision option. In all the docking runs, the exhaustiveness level was set to 8. Important interacting residues in TRPV1 for capsazepine and capsaicin binding were used to validate the docking of human TRPV1 performed in the current study. For the docking of 25OHD to human TRPV1, the first five poses, with the lowest relative free energies (ΔG), shared very similar ligand binding sites, although these binding sites were different from that of capsazepine and capscaicin. Therefore, we chose to illustrate only one binding pose in this current study. The 25OHD interacting residues from the top five poses are listed in Table 2. To further, visualize the human TRPV1-ligand complexes in a lipid milieu, VMD software was used (https://www.ks.uiuc.edu/Research/vmd/). The protein–ligand complexes were embedded into a pre-equilibrated 1-palmitoyl-2-oleoyl-sn-glycero-3-phosphatidylcholine (POPC) lipid bilayer, under periodic boundary conditions. The membrane protein complex was inserted into the bilayer after removal of lipid molecules within 3 Å of the protein. A similar strategy was undertaken for water molecules for which a TIP3P water box was used. The size of the water lipid box was 150 Å^3. The human TRPV1–ligand complex assembled within the POPC bilayer was used for further analysis. Atomistic level interactions between each ligand and hTRPV1 were visualized with LIGPLOT (Wallace *et al.* 1995).

Table 2. Human TRPV1 residues that are predicted to interact with 25OHD

Ligand pose	First protomer	Second protomer
1	Phe522, Phe543, Leu547, Met581	Ile662, Leu665, Ala666, Ile669, Leu670
2	Phe543, Ala546, Leu547, Met581	Phe591, Leu665, Ala666, Ile669, Leu670
3	Phe522, Phe543, Leu547	Phe591, Ile662, Leu663, Ala666, Leu670,
4	Phe522, Phe543, Leu547	Phe591, Ile662, Leu663, Ala666, Leu670
5	Phe543, Ala546, Leu547, Met581	Phe591, Leu663, Leu665, Ala666, Ile669, Leu670

The top five poses of the 25OHD interactions with the lowest values of negative ΔG (free energy) are listed.

Flow cytometry

Fluorochrome-conjugated and anti-cytokine antibodies were purchased from eBioscience, BioLegend, or BD PharMingen (San Diego, CA, USA). Purified $CD4^+$ naïve T-cells were stained with antibodies in a fluorescence-activated cell sorting (FACS) buffer containing $1\times$ phosphate-buffered saline (PBS), 1% fetal bovine serum, 0.02% sodium azide for 30 min on ice. Cells were then washed three times with FACS buffer after primary and secondary antibody staining. For intracellular antibody staining, cells were treated with BD Cytofix/Cytoperm (BD Biosciences). Flow cytometry was then performed on a BD LSRFortessa cell analyser, and data were then analysed with FlowJo software.

Trigeminal neuron isolation and Ca^{2+} imaging

C57BL/6J (WT) mice were obtained from Janvier Labs (Le Genest-Saint-Isle, France). All animal experiments were carried out in accordance with the European Union Community Council guidelines and were approved by the animal ethics committee of KULeuven. Trigeminal ganglia were bilaterally excised, washed in basal medium (Neurobasal A medium with 10% fetal bovine serum) and then incubated for at 37°C in media containing 1 mg ml^{-1} collagenase and 2.5 mg ml^{-1} dispase (Thermo Fisher Scientific, Ghent, Belgium). Digested ganglia were gently washed twice with media and mechanically dissociated. Neurons were seeded on poly-L-ornithine/laminin-coated glass bottom chambers (Fluorodish, WPI, Hitchin, UK) and cultured for 12–18 h at 37°C in B27 supplemented Neurobasal A medium (Thermo Fisher Scientific) containing glial cell-derived neurotrophic factor, 2 ng ml^{-1} (Thermo Fisher Scientific) and neurotrophin 4, 10 ng ml^{-1} (Peprotech, London, UK).

For Ca^{2+} imaging, cultured trigeminal neurons were loaded with 2 μM Fura2-AM ester at 37°C, 30 min prior to experimentation. Fluorescence signals were evoked during alternating excitation at 340 and 380 nm using a Lambda XL illuminator (Sutter Instruments, Novato, CA, USA), and recorded using an Orca Flash 4.0 camera (Hamamatsu, Bridgewater NJ, USA) on a Nikon Eclipse Ti fluorescence microscope (Nikon, Tokyo, Japan). The imaging data were recorded at room temperature and analysed using Nikon NIS-elements software. Emitted fluorescence at 520 nm was measured during 340 and 380 nm excitation, and after correction for the individual background fluorescence signals, the fluorescence ratio of the (F_{340}/F_{380}) was monitored and expressed graphically as relative fluorescence changes or absolute intracellular Ca^{2+} levels. TRPV1-positive neurons were identified by their sensitivity to 10 μM capsaicin.

Data analysis

GraphPad Prism 5.0 (GraphPad Software Inc., La Jolla, CA, USA) and Origin 9.0 (OriginLab Corp., Northampton, MA, USA) software were used to analyse the data. IC_{50} of dose–response curves were calculated by $y = \min + \{(\max - \min)/1 + (x/IC_{50})^n\}$, where n is the Hill coefficient. Details of the statistical analysis and grouped data numbers can be found in the figure legends. All values provided are means $\pm$ standard deviation (SD).

Results

Vitamin D is a partial agonist of TRPV1

As vitamin D shares some structural similarities and properties to agonists and antagonists of TRPV1 (Fig. 1*A*), we tested whether vitamin D directly regulates TRPV1 activity by measuring acute TRPV1-mediated calcium influx using real-time live cell imaging of HEK293T cells overexpressing human TRPV1. As expected, capsaicin elicited a robust concentration-dependent calcium influx (1 nM to 10 μM capsaicin, Fig. 1*B*). To test the effects of vitamin D we used 25OHD at 100 nM, a concentration that is in the physiological range for this major circulating vitamin D isoform (Hollis, 2005; Holick, 2007). Application of 25OHD alone elicited a small but measurable calcium influx that was ∼10% of the maximal capsaicin response (Fig. 1*C*). In the presence of 25OHD, application of 1 nM capsaicin resulted in a significant enhancement of the calcium response when compared to 1 nM capsaicin alone and this effect of 25OHD was only observed at the lower capsaicin concentrations (Fig. 1*C* and *D*). Moreover, in the

presence of 25OHD, application of capsaicin resulted in a reduction in intracellular calcium over time as denoted by the calculated negative slope of the fluorescence signal ($-\mathrm{d}F/\mathrm{d}t$, Fig. 1*C* and *E*). Taken together, these results suggest that 25OHD alone is able to activate TRPV1 and

that, at low concentrations of the full TRPV1 agonist capsaicin, TRPV1 activity is enhanced in the presence of 25OHD, whereas at higher concentrations of capsaicin, 25OHD reduces the slope of calcium influx. These findings are consistent with 25OHD being a partial agonist of
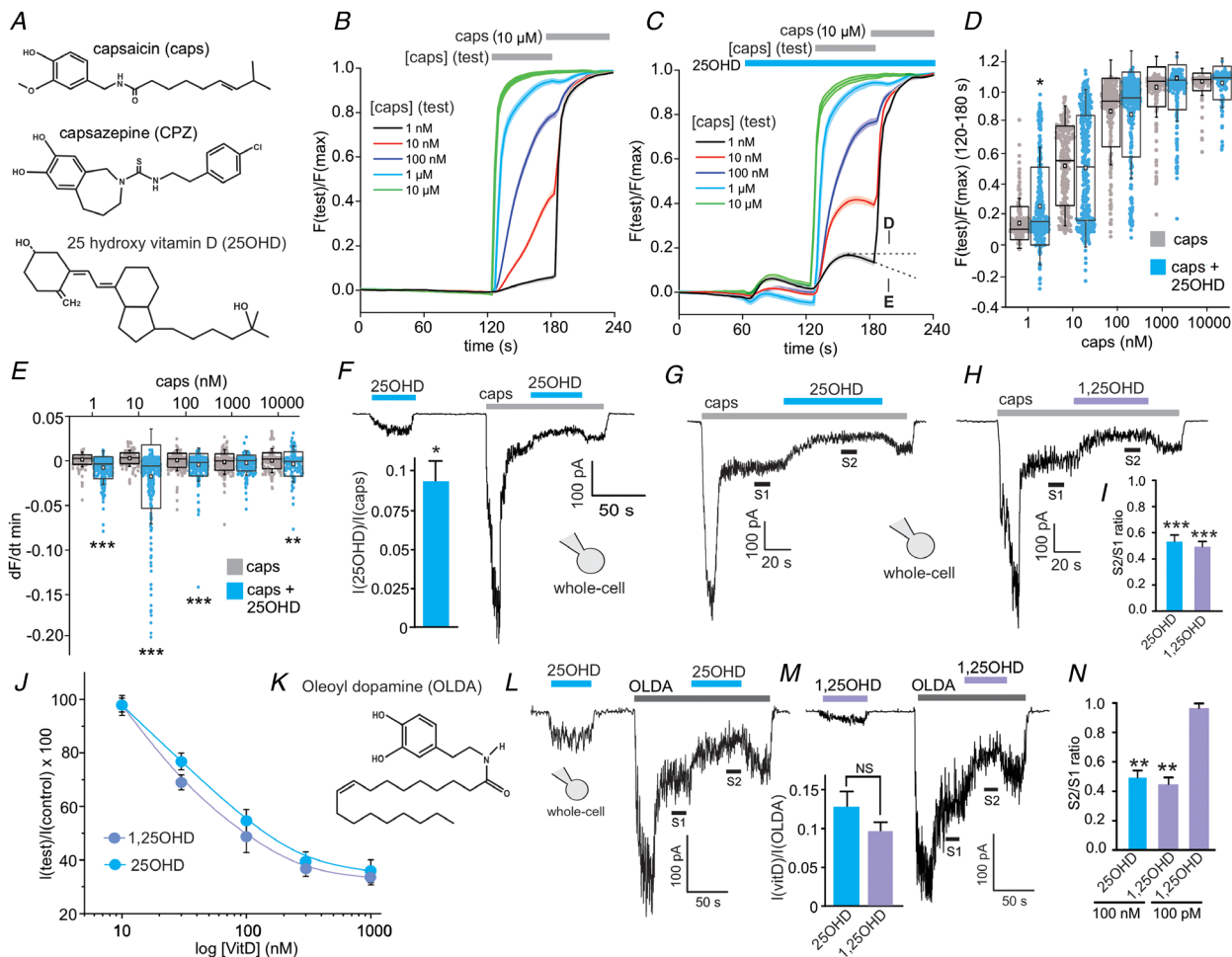
Figure 1. 25OHD is a partial agonist of TRPV1
A, chemical structures of capsaicin (caps), capsazepine (CPZ) and 25 hydroxyvitamin D (25OHD). *B* and *C*, grouped calcium imaging data illustrating the effects of capsaicin alone (1 nM to 1 μM, *B*) and 25OHD (100 nM) alone or with capsaicin (*C*) on TRPV1-mediated calcium influx (Each line represents the average fluorescence signal ($F_{\text{test}}/F_{\text{max}}$) from 150–400 cells per condition from 3–4 transfections.) *D* and *E*, grouped data analysis of *B* and *C* showing the effects of 25OHD (100 nM) on peak TRPV1-mediated calcium influx (*D*) and the negative slope of the calcium signal (d*F*/d*T*, *E*). Data presented as quartiles 1–3 boxplots with mean (white square), median (horizonal line) and standard deviation (whiskers). *F*, representative TRPV1 whole-cell current recordings of the effects of 25OHD (100 nM) alone or after activation with capsaicin. Bar graph inset shows the ratio of 25OHD-induced peak current/capsaicin induced peak current (0.1 ± 0.02). *G* and *H*, representative TRPV1 whole-cell current recording illustrating that 25OHD and 1,25OHD (100 nM) inhibit (S2) the capsaicin-induced TRPV1 current (S1). *I*, grouped S2/S1 ratio data for *G* and *H*. *J*, concentration–inhibition curves for the effects of 25OHD and 1,25OHD on capsaicin-induced whole-cell TRPV1 currents ($IC_{50} = 34.3 \pm 0.2$ and 11.5 ± 0.9 nM, respectively). *K*, structure of *N*-oleoyldopamine (OLDA). *L* and *M*, representative TRPV1 whole-cell current recording illustrating that 25OHD (*L*) and 1,25OHD (*M*) inhibit the TRPV1 current elicited by OLDA (1 μM). *M*, subpanel: grouped data showing the weak partial agonist effect of 100 nM 25OHD and 1,25OHD when compared to the maximal effect of OLDA (1 μM). *N*, grouped data for *L* and *M* with S2/S1 ratio as 0.49 ± 0.1 and 0.45 ± 0.05 for 25OHD and 1,25OHD, respectively (note that 100 pM 1,25OHD was without effect, representative trace not shown). All experiments were performed in HEK293T cells overexpressing recombinant human TRPV1. Grouped data for the whole-cell current data are mean ± SD values from $n = 3$–6 cells per group. Statistical analysis was performed by Student's *t* test: *$P < 0.05$, **$P < 0.01$, ***$P < 0.005$; NS, no significant difference. [Colour figure can be viewed at wileyonlinelibrary.com]

TRPV1. To provide further evidence of this partial agonist concept, we employed a different experimental system by measuring whole-cell currents from HEK293T cells expressing TRPV1. Application of 100 nM 25OHD alone resulted in activation of TRPV1 that was ∼10% of the maximal capsaicin response (Fig. 1*F*), a value similar to the calcium imaging data (Fig. 1*C*). Interestingly, 25OHD did not result in any measurable calcium-induced desensitization that is commonly observed with full agonists of TRPV1 such as capsaicin (Fig. 1*F*). However, in the presence of 1 μM capsaicin, 25OHD and 1,25OHD (100 nM) significantly reduced the sustained steady-state TRPV1 current with a S2/S1 ratio of 0.6 ± 0.08 and 0.5 ± 0.1 respectively (Fig. 1*G–I*). The IC$_{50}$ values for this inhibitory effect were 34.3 ± 0.2 and 11.5 ± 0.9 nM for 25OHD and 1,25OHD, respectively (Fig. 1*J*). As capsaicin is an exogenous TRPV1 full agonist, we investigated whether 25OHD was similarly able to inhibit the stimulatory effects of a known endogenous TRPV1 full agonist, OLDA (Fig. 1*K*) (Chu *et al.* 2003; Zhong & Wang, 2008). Application of 100 nM 25OHD or 1,25OHD produced an equipotent weak activation of TRPV1 that was ∼10% of the maximal OLDA (1 μM) response (Fig. 1*L* and *M*). OLDA elicited whole-cell currents that displayed similar kinetics to that observed with capsaicin, consisting of a transient peak current and a sustained desensitization resistant steady-state current (Fig. 1*L* and *M*). During this sustained current (S1), application of 100 nM 25OHD or 1,25OHD resulted in a significant inhibition of the current (S2) with S2/S1 ratio of 0.49 ± 0.1 and 0.45 ± 0.05, respectively (Fig. 1*L–N*), of a similar magnitude to that observed with capsaicin (Fig. 1*I*). A lower concentration of 100 pM 1,25OHD showed no effect on OLDA induced currents. (Fig. 1*N*, representative current trace not shown).

In order to study the kinetics of the 25OHD partial agonist effect in more detail, we performed single channel analysis of TRPV1 using the cell-attached patch-clamp technique. Application of 100 nM 25OHD (1) modestly increased the time spent in the open state (τ) (Fig. 2*B*, τ (vehicle) = 67 ms and τ (25OHD) = 81 ms), (2) increased the frequency of single TRPV1 channel opening (Fig. 2*B* inset, vehicle = 0.35 and 25OHD = 0.64 events/s), and (3) the open probability (P_o) (Fig. 2*C*, P_o for 25OHD = 6.4 ± 4.8-fold increase compared to vehicle). As expected, application of capsaicin (1 μM) caused a robust increase in TRPV1 open probability, whereas co-application of 25OHD significantly reduced TRPV1 open probability by decreasing the number of channel openings (Fig. 2*D* and *F*, P_o (caps/25OHD) = 0.6 ± 0.1) compared to capsaicin application only. Interestingly, in the presence of capsaicin, 25OHD may still be able to stabilize the open state of TRPV1 channels as there was a slight increase in the time spent in the open state (τ) (Fig. 2*E*, τ (caps) = 110 ms *vs.* τ (caps/25OHD) = 139 ms)

while reducing the frequency of open events (Fig. 2*E* inset, caps = 2.56 *vs.* caps/25OHD = 1.25 open events/s). Together these results may explain the observed effect of 25OHD antagonizing the agonist effects of capsaicin with respect to open probability (Fig. 2*F*). The unitary current amplitude (UCA) of open TRPV1 channels remained unchanged in the presence of 25OHD (Fig. 2*G*, UCA (caps) = 4.3 pA *vs.* UCA (25OHD) = 4.1 pA). These results indicate that 25OHD increases TRPV1 open probability by stabilizing the open state and increasing the open probability of TRPV1 channels. Taken together these single channel results are also consistent with 25OHD being a partial agonist of TRPV1.

To gain further insights into where in the TRPV1 channel complex 25OHD is acting, we sought to determine whether 25OHD can also antagonize the effects of another known TRPV1 activator, low pH, which opens TRPV1 by a mechanism independent of the documented vanilloid capsaicin binding pocket within TRPV1. Using the whole-cell TRPV1 current technique, we utilized a paired pulse protocol (Fig. 3*A* and *C*) that measures the effects of capsaicin, 25OHD or low pH in same population of channels while allowing for correction of the known desensitization of TRPV1 that occurs with repeated agonist application. Sequential paired activation of TRPV1 with capsaicin resulted in a ∼50% reduction in whole-cell current during the second pulse when compared to the first pulse (P2/P1, Fig. 3*A* and *B*). As expected, when 25OHD was co-applied with capsaicin during the second pulse, the peak current was significantly reduced (Fig. 3*A* and *B*) when compared to capsaicin alone (P2/P1 (caps) = 0.55 ± 0.06 *vs.* P2/P1 (caps+25OHD) = 0.27 ± 0.05). Application of a low pH solution (pH 5.5) resulted in the induction of a slowly developing TRPV1 current (Fig. 3*C*). In contrast to capsaicin, co-application of 25OHD with a pH 5.5 solution did not further reduce the magnitude of the induced TRPV1 current (Fig. 3*C*, P2/P1 (pH 5.5) = 0.46 ± 0.05 *vs.* P2/P1 (pH 5.5+25OHD) = 0.51 ± 0.07, Fig 3*D*). As expected from our earlier experiments, the application of 100 nM 25OHD alone induced partial activation of TRPV1 currents, but 25OHD did not alter the steady-state TRPV1 currents induced by pH 5.5 (Fig. 3*E–G*). These results indicate that 25OHD is acting as a competitive antagonist of capsaicin, but not low pH, suggesting that the 25OHD binding site may be situated in the same capsaicin vanilloid binding pocket within TRPV1.

25OHD binds in a similar region within TRPV1 as capsaicin and capsazepine

In order to further explore the putative binding site(s) for 25OHD within the TRPV1 complex, we generated a homology model of TRPV1 based on the cryo-EM structure of rat TRPV1 (Liao *et al.* 2013), which

shares 86% sequence identity to human TRPV1. We then employed an algorithm-based modelling method followed by molecular docking to gain insights into where 25OHD may bind to the TRPV1 in relation to the known binding sites for the agonist capsaicin and the antagonist capsazepine (Szallasi *et al.* 2007; Yang *et al.* 2015). Consistent with these previous docking studies, we observed that the vanilloid groups of both capsaicin and capsazepine were oriented parallel to the S4–S5 linker with possible hydrogen bond interactions with residues Y511 and S512 (Fig. 4*A–F*). The amide groups of these two ligands are predicted to interact with T550 with the tails of these two ligands oriented upwards in the binding pocket Fig. 4*C* and *F*). Residues L553 and E570 are also predicted to have interactions with capsaicin and capsazepine (Fig. 4*C* and *F*).

Our modelling data predict that 25OHD binds within the same region as both capsaicin and capsazepine, with the binding pocket consisting of residues from the two protomers of the homodimer (Fig. 4*G–I*). However, 25OHD exhibits a different binding pose within this vanilloid binding pocket, as the aromatic group of 25OHD is not predicted to interact closely with known capsaicin-interacting residues within the vanilloid domain with no close interactions predicted with residues Y511 and S512. Our modelling predicts that 25OHD binding is perpendicular to the other two ligands with both its head and tail situated in the upper binding pocket (Fig. 4*H* and *I*). The observation that additional residues from the second protomer are involved in 25OHD binding suggests that the binding of 25OHD to these residues could lead to a conformational change to elicit channel gating (i.e. partial agonism). This conformational change may also (1) facilitate 25OHD interactions with Y511 and S512 that are known capsaicin binding residues or (2) alter the position of these two residues. One or both of these putative mechanisms may reduce the partial agonism of TRPV1 by 25OHD and decrease the potency of capsaicin
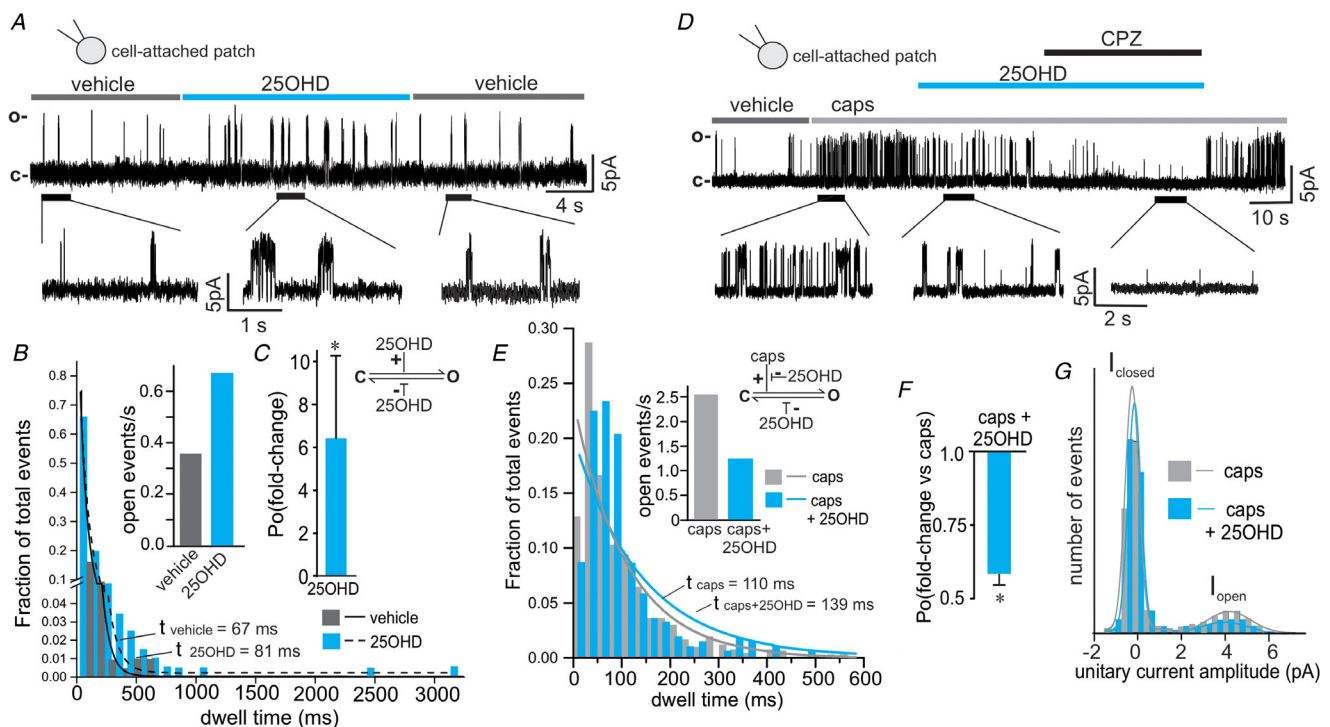
Figure 2. TRPV1 single channel kinetic analysis
A, representative single channel current recording of TRPV1 and the effects of 100 nM 25OHD using the cell-attached patch-clamp mode. *B* and *C*, single channel analysis illustrating that 100 nM 25OHD increases the time spent in the open state (dwell time) and the frequency of open events (*B*), resulting in a significant 6.4 ± 4.8-fold increase in open probability (*C*, $n = 5$ cells). *D*, representative TRPV1 single channel current recording illustrating the inhibitory effects of 100 nM 25OHD and 1 μM capsazepine (CPZ) on currents induced by capsaicin (caps) using the cell-attached patch-clamp mode. *E* and *F*, single channel analysis illustrating that 100 nM 25OHD is still able to increase the time spent in the open state (dwell time) although the frequency of channel opening is reduced (inset graph), resulting in a significant reduction in open probability (P_o) (caps/25OHD $= 0.6 \pm 0.1$-fold change, $n = 4$ cells, *F*). *G*, unitary current amplitude histogram of 1 μM capsaicin-induced TRPV1 single channel activity (open state amplitude $= 4.3$ and 4.1 pA for caps and 25OHD, respectively). Channel open dwell time and opening events per second are presented as total absolute number of all the events collected. Statistical analysis was performed with a paired Student's *t* test, *$P < 0.05$. [Colour figure can be viewed at wileyonlinelibrary.com]
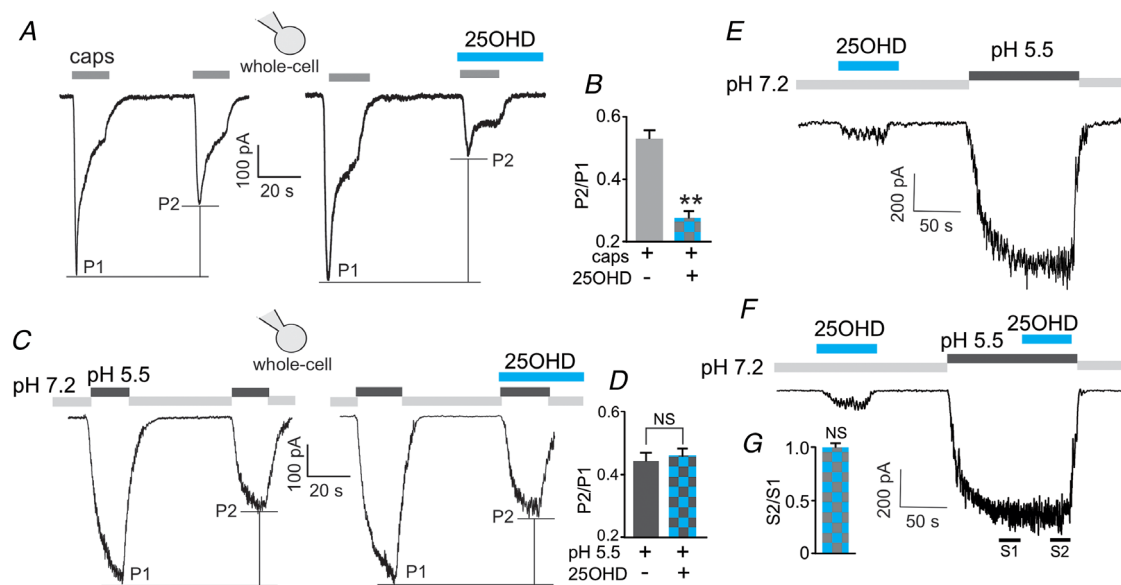
agonism in the presence of 25OHD, accounting for the observed competitive antagonist effects of 25OHD.

To test the predicted 25OHD binding sites experimentally, we employed an alanine substitution approach to mutate predicted ligand interacting residues. Accordingly, we generated Y511A, S512A, T550A, L553A and E570A point mutations in the human TRPV1 sequence and then measured the mutant TRPV1 current responses to capsaicin and 25OHD using the whole-cell patch-clamp technique. To test the partial TRPV1 agonist effects, 25OHD was applied to elicit TRPV1 currents from wild-type (WT) or mutant channels. The stimulatory effect of 25OHD on TRPV1 was almost completely abolished in Y511A and S512A mutant channels when compared to WT, whereas it was unaffected in the T550A, L553A and E570A mutants (Fig. 5A–G). Furthermore, the competitive antagonist effects of 25OHD on capsaicin-induced currents were only reduced in the Y511A and S512A TRPV1 mutant channels (Fig. 5A–G and I). With respect to the capsaicin sensitivity in TRPV1 channels containing these point mutations, the magnitude of capsaicin-induced current was significantly reduced in all mutants except L553A when compared to WT TRPV1 channels (Fig. 5H). Cell-attached recordings of single TRPV1 channel activity demonstrated that the 25OHD-induced increase in open probability (P_o) of TRPV1 channels containing

either the Y511A or S512A mutation was abolished (Fig. 5J–M, P_o (Y511A-25OHD) = 0.9 ± 0.1 and P_o (S512A-25OHD) = 1.0 ± 0.1 compared to P_o (WT-25OHD) = 6.4 ± 4.8). Taken together, these results validate our *in silico* modelling data as other groups have similarly identified the same capsaicin-interacting residues within the vanilloid binding pocket (Liao *et al.* 2013). Furthermore, our results also suggest that the key residues Y511 and S512 are also important for mediating the observed partial agonist and antagonist effects of 25OHD on TRPV1.

25OHD reduces the TRPV1 stimulatory effects of protein kinase C

Phosphorylation of TRPV1 by protein kinase C (PKC) is a documented mechanism by which TRPV1 activity can be potentiated (Bhave *et al.* 2003; Mandadi *et al.* 2004; Studer & McNaughton, 2010). Therefore, we tested whether 25OHD may regulate PKC-mediated TRPV1 activity. Using the cell-attached technique to record single TRPV1 channel currents, application of the PKC activator phorbol 12-myristate 13-acetate (PMA, 1 µM) during capsaicin agonism resulted in a significant increase in the fold change in P_o (Fig. 6A and C, P_o (caps/PMA) = 2.2 ± 0.5, when compared to capsaicin alone). In the presence of capsaicin (1µM), 25OHD (100 nM) significantly reduced the

Figure 3. Vitamin D does not inhibit low pH-induced TRPV1 currents
A and *B*, representative whole-cell current recording (*A*) and grouped data (*B*) of macroscopic TRPV1 currents, using a paired pulse protocol (P2/P1), illustrating that 25OHD (100 nM) significantly inhibits TRPV1 currents induced by 1 µM capsaicin (P2/P1 ratios for capsaicin only and capsaicin+25OHD are 0.55 ± 0.06 and 0.27 ± 0.05, respectively, *n* = 6–8 cells). *C*, in contrast, 25OHD did not reduce TRPV1 currents induced by low pH (pH 5.5). *D*, the P2/P1 ratio for pH 5.5 and pH 5.5+25OHD = 0.46 ± 0.05 and 0.51 ± 0.07, respectively, *n* = 4–6 cells per group. *E* and *F*, 25OHD alone partially activates TRPV1 currents. *F* and *G*, application of 25OHD during the steady-state phase of the pH 5.5-induced current did not significantly TRPV1 activity (S2/S1 ratio). *n* = 4–6 cells per group. **P < 0.01; NS, no significant difference. [Colour figure can be viewed at wileyonlinelibrary.com]

TRPV1 P_o with PMA being unable to potentiate TRPV1 activity (Fig. 6B and C, P_o (caps/25OHD) = −0.42 ± 0.1 and P_o (caps/25OHD/PMA) = 0.24 ± 0.2, when compared to capsaicin alone). To determine the effects of capsaicin, 25OHD and PMA in a macroscopic population of channels, we measured whole-cell TRPV1 currents utilizing the paired pulse protocol. PMA significantly increased the magnitude of the TRPV1 current induced by capsaicin, but co-application of PMA and 25OHD prevented this PMA-induced potentiation of current (Fig. 6D and E, normalized P2/P1 ratios:

caps/PMA = 1.8 ± 0.08, caps/PMA/25OHD = 1.3 ± 0.05, when compared to capsaicin alone). While this result suggests 25OHD may directly interfere with the actions of PKC on TRPV1, it could also be explained by 25OHD inhibiting the capsaicin-induced current, as we previously observed (Fig. 2H), in a PKC-independent manner. Therefore, to explore the mechanism further, we generated alanine-substituted point mutations at three documented PKC phospho-acceptor residues: S502A, T704A and S800A (Numazaki *et al.* 2002; Wang *et al.* 2015). As previously shown in Fig. 1F, 25OHD significantly
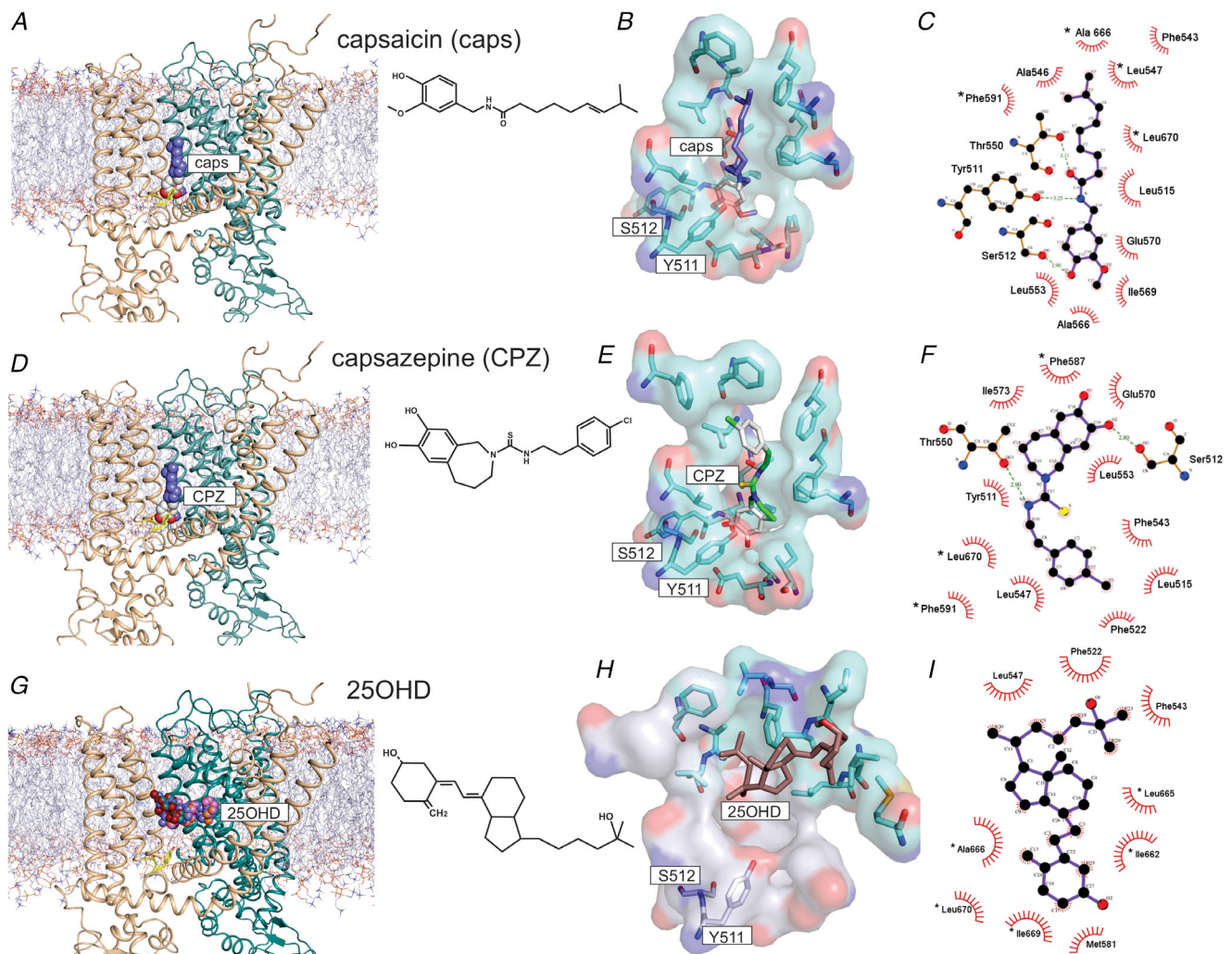
**Figure 4. 3D modelling and ligand docking to human TRPV1**

A, *D* and *G*, docking results for capsaicin (*A*), capsazepine (*D*) and 25OHD (*G*). A homodimer model (protomer 1, wheat colour; protomer 2, teal colour) embedded in a POPC bilayer is shown. The molecules are shown as spherical form and colour-coded by elements. *B*, *E* and *H*, the docking of these molecules represented as surface plots. The head and tail groups of capsaicin are shown in white and purple respectively. Capsazepine is shown with hydrophobic groups in white and charged residues coloured. 25OHD is shown in brown with its putative binding pocket coloured cyan *versus* the capsaicin/capsazepine binding pocket coloured light grey. The oxygen and nitrogen atoms in TRPV1 are shown as red and blue surfaces. TRPV1 interacting residues are labelled and shown in stick format. *C*, *F* and *I*, Ligplot binding pocket analysis for capsaicin (*C*), capsazepine (*F*) and 25OHD (*I*). Green dashed lines indicate hydrogen-bonding interactions with red line curves indicating hydrophobic interactions pairs of atoms. *Residues belonging to the 2nd protomer. [Colour figure can be viewed at wileyonlinelibrary.com]

reduced the magnitude of capsaicin-induced sustained whole-cell currents in WT TRPV1 channels (Fig. 6F–J). We observed similar inhibitory effects of 25OHD in WT TRPV1 channels and the mutant T704A and S801A channels (Fig. 6F and H–J, normalized S2/S1 ratio for WT = 0.4 ± 0.04, T704A = 0.5 ± 0.09, S801A = 0.5 ± 0.08). However, the inhibitory effects of 25OHD on the capsaicin-induced current were completely abolished in the S502A mutant (Fig. 6G and J, normalized S2/S1 ratio = 0.8 ± 0.05). Taken together, these results suggest that there may be either significant direct or allosteric interactions between 25OHD and the serine at

position 502, which is located at the base of the vanilloid binding pocket (Fig. 5K).

Vitamin D reduces CD4+ T-cell activation and TRPV1-mediated calcium entry into neurons

Our results so far indicate that vitamin D is a novel modulator of TRPV1 but whether this observation has physiological relevance remains to be tested. Therefore, we explored this concept using two *in vitro* primary cell models where TRPV1 activity plays an important role in cellular function, namely CD4+ T-cell activation and
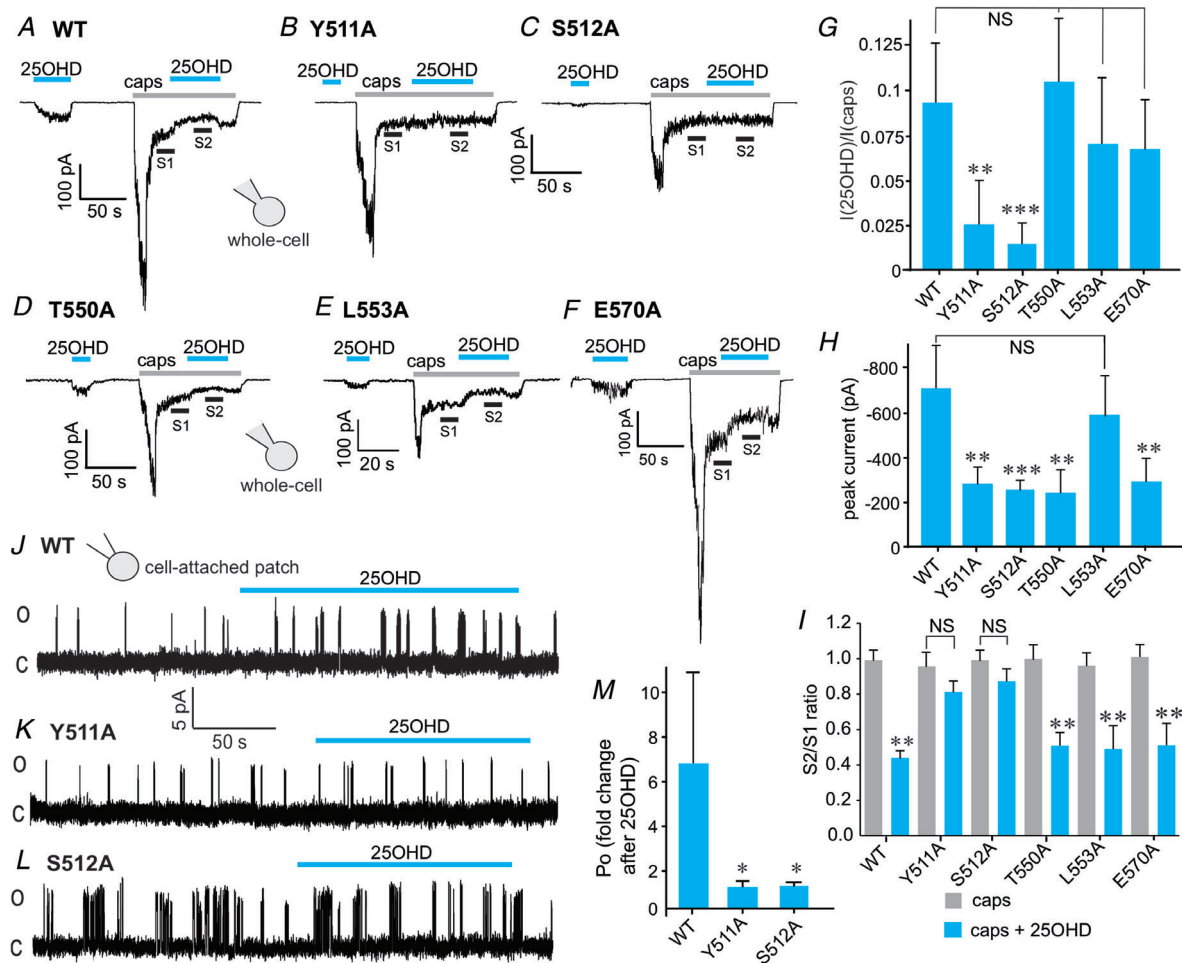
Figure 5. Y511 and S512 are 25OHD interacting residues
A–F, representative traces of whole-cell current (WT) elicited by 100 nM 25OHD and the inhibition of 1 μM capsaicin-induced sustained current by 25OHD (100 nM) in WT (*A*), and the Y511A (*B*), S512A (*C*), T550A (*D*), L553A (*E*) and E570A (*F*) TRPV1 mutants. *G*, normalized grouped data illustrating that the agonist effect of 25OHD (100 nM) is significantly reduced in the Y511A and S512A mutants. *H*, normalized grouped data of the ratio (S2/S1) of the sustained capsaicin-induced currents before (S1) and during (S2) 25OHD application in WT and mutant TRPV1 whole-cell currents ($n = 3–5$ cells per group). *J–L*, representative recordings of the effects of 25OHD (100 nM) on single channel currents from TRPV1 WT, Y511A and S512A TRPV1 mutants. *M*, normalized grouped data illustrating that the stimulatory effects of 25OHD (fold change in $P_o = 6.4 \pm 4.8$) on open probability are significantly reduced by ~6-fold in the Y511A (fold change in $P_o = 0.93 \pm 0.1$) and S512A (fold change in $P_o = 1 \pm 0.1$) TRPV1 mutants. Grouped data values are means ± SD ($n = 4–6$ cells per group). *$P < 0.05$, **$P < 0.01$, ***$P < 0.005$, paired Student's *t* test; NS, no significant difference. [Colour figure can be viewed at wileyonlinelibrary.com]

TRPV1-induced calcium influx in cultured trigeminal neurons. TRPV1 activity has been shown to be important in the activation of CD4^{+} T-cells (Bertin *et al.* 2014). Using flow cytometry, we tested whether 25OHD and 1,25OHD regulated cytokine production from enriched mouse CD4^{+} T-cells. Treatment with the known TRPV1 antagonist capsazepine (CPZ, 5 μM) significantly reduced the frequency of TNFα and INFγ double positive CD4^{+} T-cells by 76.2 ± 7.2, after 24 h activation by plate-bound anti-CD3 and anti-CD28 antibodies. This result confirms

that TRPV1 activity is important for T-cell activation in our model system (Fig. 7*A* and *B*). Furthermore, treatment of CD4^{+} T-cells with 25OHD or 1,25OHD (100 nM) also significantly reduced the frequency of TNFα and INFγ double positive CD4^{+} T-cells ($25.3 \pm 23.1\%$ and $34.4 \pm 14.4\%$, respectively, Fig. 7*A* and *B*), albeit to a lesser extent than CPZ.

Trigeminal neurons involved in the transduction of nociceptive signals are known to express TRPV1. Therefore, we tested whether 25OHD may attenuate
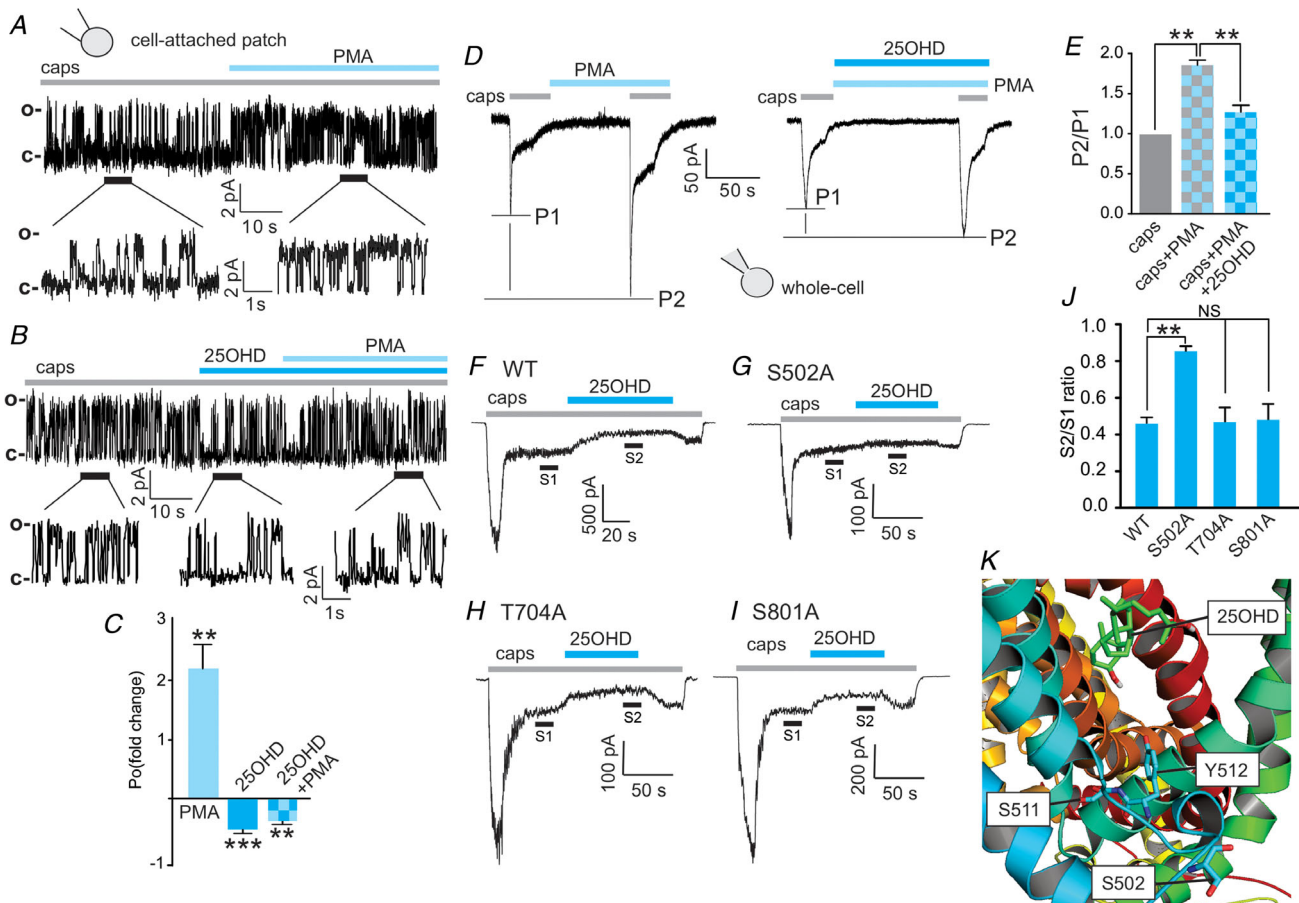
Figure 6. The TRPV1 phospho-acceptor residue S502 mediates the inhibitory effects of 25OHD on PKC-induced potentiation of TRPV1 activity

A and *B*, representative cell-attached patch single-channel recordings showing that the PKC activator phorbol 12-myristate 13-acetate (PMA, 1 μM) potentiates the increases in open probability of WT TRPV1 single channel currents induced by capsaicin (1 μM) (*A*) and that co-application of 25OHD (100 nM) with PMA prevents this potentiation (*B*). *C*, grouped data from *A* and *B* showing fold changes in open probability (P_o) (caps+PMA = 2.2 ± 0.5, caps+25OHD = 0.42 ± 0.1, caps+25OHD+PMA = 0.24 ± 0.2, $n = 6$ patches per group). *D* and *E*, representative whole-cell current recordings, using a paired pulse protocol, illustrating that PMA potentiates the capsaicin-elicited current and that 25OHD significantly reduces the PMA potentiating effect. *E*, grouped data (normalized to capsaicin alone) of the P2/P1 ratio for caps/PMA and caps/PMA/25OHD: 1.8 ± 0.08 and 1.3 ± 0.05, respectively ($n = 5$–6 cells per group). *F*–*I*, representative whole-cell current traces from WT, S502A, T704A and S800A mutants illustrating that the inhibitory effects of 25OHD on PMA potentiation of sustained TRPV1 currents are significantly reduced only in the S502A mutant. *J*, normalized grouped data from *F*–*I*. S2/S1 ratios for WT, S502A, T704 and S801A are 0.4 ± 0.04, 0.8 ± 0.05, 0.5 ± 0.09 and 0.5 ± 0.08, respectively ($n = 5$–7 cells per group, mean $\pm$ SD). *K*, human TRPV1 homology 3D model illustrating the predicted locations of S502 in relation to Y511 and S512 and the putative 25OHD binding site. Statistical analysis was performed with a paired Student's *t* test: **$P < 0.01$, ***$P < 0.005$ respectively; NS, no significant difference. [Colour figure can be viewed at wileyonlinelibrary.com]

capsaicin-induced calcium influx in isolated trigeminal neurons. As TRPV1 desensitizes at high concentrations of capsaicin, a low concentration of capsaicin (10 nM) was used to elicit measurable submaximal TRPV1-mediated calcium influx into neurons. To identify TRPV1 positive neurons within the cell population, we applied 10 μM capsaicin at the end of each experimental run and determined that 43% (169/389) of neurons expressed functional TRPV1 channels (Fig. 7C). Application of the low concentration of capsaicin (10 nM) evoked a measurable calcium influx in 12% (20/169) of the TRPV1$^+$ neurons. While application of 25OHD (100 nM) alone did not result in significant increases in calcium influx,

the capsaicin-induced calcium influx was significantly reduced by 33% in the presence of 25OHD compared to capsaicin alone (Fig. 7D, caps = 199.8 ± 155.4 nM; 25OHD/caps = 108.6 ± 50.6 nM, 25OHD = 74.7 ± 19.4 nM). Normalized data (to caps) are presented in Fig. 7E (25OHD/caps = 0.68 ± 0.26 and 25OHD = 0.51 ± 0.24).

Discussion

Since the initial discovery of TRPV1 as the elusive molecular receptor for capsaicin (Caterina *et al.* 1997), it has been shown that TRPV1 activity can be
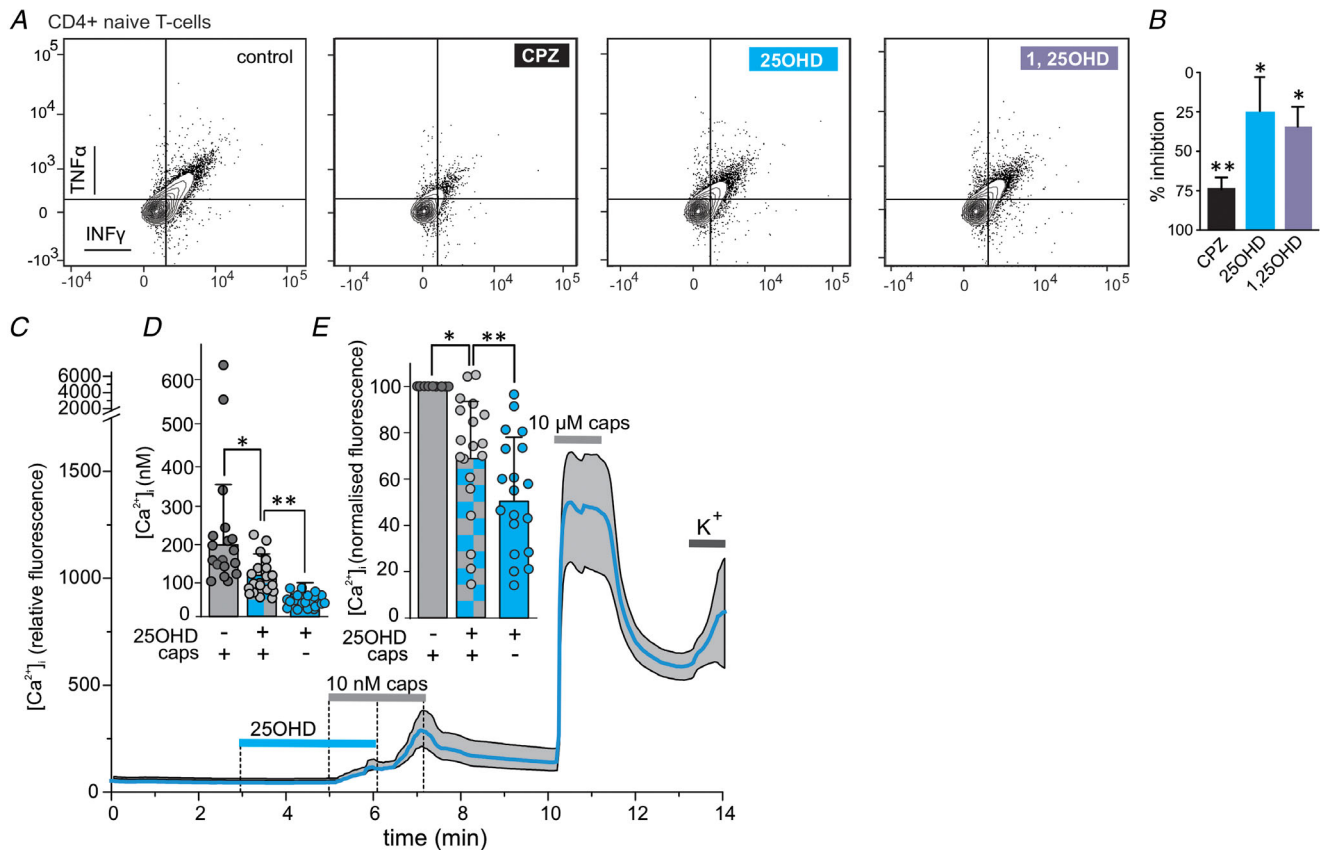
Figure 7. Regulation of cellular function mediated by TRPV1

A, flow cytometry analysis of enriched CD4$^+$ T-cells illustrating that the TRPV1 antagonist capsazepine (CPZ, 1 μM), 25OHD (100 nM) and 1,25OHD (100 nM) reduces the production of the cytokines TNFα and IFNγ. *B*, grouped data from *A* showing percentage of inhibition of TNFα/IFNγ production by CPZ (76.2 ± 7.2%), 25OHD (25.3 ± 23.1%) and 1,25OHD (34.4 ± 14.4%). *P < 0.05, **P < 0.01, one-way ANOVA (*n* = 4 experiments per group). *C*, representative calcium-imaging traces from TRPV1$^+$ trigeminal neurons and the effects of 25OHD and capsaicin (blue line and grey shaded area show mean and SD, respectively). *D* and *E*, grouped calcium imaging data from *C* expressed as either calculated calcium concentration (*D*, caps = 199.8 ± 155.4 nM, 25OHD+caps = 108.6 ± 50.6 nM and 25OHD 74.7 ± 19.4 nM) or normalized calcium signal (*E*, caps = 1.0, 25OHD+caps = 0.68 ± 0.26 and 25OHD = 0.51 ± 0.24). 25OHD (1 μM) significantly reduces the stimulatory effects of capsaicin (caps, 10 nM) by ∼33%. *P < 0.05, **P < 0.01 (mean ± SD; paired sample *t* test, *n* = 19 neurons, 5 individual recordings). Note, a low concentration of caps (10 nM) only evoked a measurable calcium influx in 11% (19/169) of all TRPV1-expressing neurons as determined by their responsiveness to a high capsaicin concentration of 1 μM. Therefore, only these low capsaicin-sensitive neurons were included in the representative traces and statistical analysis. [Colour figure can be viewed at wileyonlinelibrary.com]

regulated by a variety of pathways including pH, heat, phosphorylation and other noxious exogenous ligands such as resiniferatoxin (Elokely *et al.* 2016). The exquisite sensitivity of TRPV1 to nanomolar concentrations of capsaicin and resiniferatoxin suggest that endogenous ligands for TRPV1 likely exist and may play an important biological role through their modulation of TRPV1 activity in a wide variety of cellular systems where TRPV1 activity is involved. In this respect, a number of endogenous TRPV1 ligands have been identified, including anandamide, oxytocin, oxidized linoleic acid metabolites, *N*-acylethanolamines and *N*-acyldopamines (e.g. OLDA), which play a role in promoting inflammatory hyperalgesia and thermal allodynia (Chu *et al.* 2003; Movahed *et al.* 2005; Zhong & Wang, 2008; Spicarova & Palecek, 2009; Green *et al.* 2013; Nerseyan *et al.* 2017). Our results now indicate that 25OHD should be added to the list of endogenous TRPV1 ligands, given its action as a partial agonist of TRPV1. While a number of naturally occurring plant-derived or synthetic partial agonists and antagonists have been characterized (Blumberg *et al.* 2011; Wang *et al.* 2016), 25OHD joins anandamide as a rare example of an endogenous partial agonist of TRPV1 (Ross, 2003). 25OHD is able to submaximally activate TRPV1 without inducing measurable calcium-induced desensitization (Fig. 1*F*), whereas 25OHD and 1,25OHD are capable of reducing capsaicin and OLDA-induced TRPV1 currents. The mechanisms by which this 25OHD partial agonism occurs are of interest and we provide evidence that 25OHD increases the frequency of single channel opening and perhaps also stabilizes the open state, resulting in an increase in channel open probability. In the presence of capsaicin, 25OHD decreases open probability by reducing the frequency of channel opening by ∼50%. Moreover, when 25OHD is co-applied with low nanomolar levels of capsaicin (1 nM), we observed an increase in TRPV1-mediated calcium influx (Fig. 1C), suggesting both molecules are acting as agonists and potentiating the actions of each other. Taken together, our results are consistent with 25OHD being a partial agonist of TRPV1.

The observation that 25OHD inhibits the effects of TRPV1 agonists but does not affect TRPV1 activation by low pH suggests 25OHD may interfere with the binding of TRPV1 agonists within the documented TRPV1 vanilloid binding pocket (Szallasi *et al.* 2007; Elokely *et al.* 2016). Protons activate TRPV1 via interactions with extracellular residues of the transmembrane segments and loops (Ryu *et al.* 2007). In contrast, agonists such as capsaicin interact with the vanilloid binding pocket located within the transmembrane domains. Therefore, it is not uncommon that TRPV1 vanilloid binding pocket agonists can activate TRPV1 without altering proton induced TRPV1 activation. Therefore, it is reasonable to suggest that 25OHD may also be interacting with the capsaicin binding sites without altering proton-induced activation.

Despite some similarities between 25OHD and known TRPV1 agonists such as lipophilicity, there are marked differences in their structures. For instance, the general characteristics of TRPV1 agonists (e.g. capsaicin) are hydrogen bond (H-bond) acceptors at the head (aryl ring) and neck position with a hydrophobic tail, which facilitate significant residue interactions within the TRPV1 binding pocket (Szallasi *et al.* 2007; Elokely *et al.* 2016). TRPV1 antagonists tend to possess more complex aromatic groups adjacent to the aryl ring in the head region, an amide/ester structure and a lipophilic tail (Szallasi *et al.* 2007). In contrast, the structure of 25OHD possesses no aryl ring or aromatic structures but contains cyclohexane and cyclopentane ring structures with a hydroxyl group at each end of the molecule. The ring structures in 25OHD are in the chair conformation, whereas the aryl ring in the full agonists is in the planar conformation, suggesting that the structure of 25OHD may be more flexible. Moreover, 25OHD is lacking the amide group in the central region of the capsaicin and capsazepine which is thought to be essential for interactions with T550 in TRPV1 since it stabilizes their position within the vanilloid binding pocket. Therefore, the less rigid structure and lack of an amide group in 25OHD suggests it may be able to move more freely within the vanilloid binding pocket. This may explain the observed reduced efficacy of 25OHD as a full agonist, where even micromolar levels of 25OHD were only partially effective in antagonizing the effects of capsaicin (Fig. 1*J*), yet still able to compete with full agonists within the binding pocket.

Further evidence for 25OHD as a TRPV1 partial agonist were gleaned from our alanine substitution experiments, in which we generated TRPV1 mutations in known capsaicin-interacting residues. Our data show that capsaicin sensitivity is reduced in the Y511A, S512A, T550A and E570A TRPV1 mutants. These results confirm the results of previous studies that highlight the importance of these residues in capsaicin binding, with Y511 being identified as a major capsaicin-interacting residue (Szallasi *et al.* 2007; Elokely *et al.* 2016). Of interest is our observation that 25OHD is no longer able to either act as a partial agonist or antagonize capsaicin-induced currents in the Y511A and S512A TRPV1 mutants (Fig. 5). As these two mutations reduce capsaicin sensitivity/binding, it may be expected that 25OHD would be a more effective capsaicin antagonist, but the opposite was observed. Therefore, these results support the notion that 25OHD may interact with Y511 and S512. One possibility is that the entry of 25OHD into the vanilloid binding channel pocket may be governed by these two residues, with mutations preventing entry. Such an interaction was not predicted from our *in silico* docking simulations and may reflect the flexibility of the 25OHD

structure and that of the TRPV1 complex itself, allowing for additional interactions not possible to effectively resolve in our ligand docking simulations. Furthermore, when known capsaicin-interacting residues were mutated, the inhibitory effects of 25OHD on capsaicin-induced TRPV1 activity were essentially the same as in WT TRPV1 currents. These observations provide further evidence that 25OHD is not binding to the exact same residues/region in the vanilloid binding as capsaicin and this is supported by the docking simulations that predict 25OHD to reside in the upper region of this binding pocket rather than in the 'head down, tail up' conformation observed for capsaicin and capsazepine (Fig. 4) (Szallasi *et al.* 2007; Elokely *et al.* 2016). As TRPV1 is a dynamic channel and our current knowledge of the ligand binding pockets is incomplete, further studies are warranted to fully characterize residues involved in 25OHD binding to the vanilloid pocket of TRPV1.

Taken together, we speculate that 25OHD may require interactions with Y511 and S512 to be guided into the vanilloid binding pocket. These interactions may lead to a minor conformational change that favours transitions into the open state. This notion is supported by our single channel kinetic analysis showing that 25OHD is able to increase the frequency of channel opening as well as stabilize the open state. With respect to phosphorylation, we determined that 25OHD prevents the PKC-mediated potentiation of capsaicin-induced TRPV1 currents. This effect seems to be dependent on the phospho-acceptor S502 residue, as an alanine substitution prevented 25OHD from antagonizing the capsaicin-induced currents in the S502A mutant. Indeed, our *in silico* modelling predicts that S502 resides between Y511 and S512 at the base of the vanilloid binding pocket, and thus S502, and its phosphorylated form, may also play a similar role to Y511 and S512 in guiding 25OHD into its active site within the pocket. Further detailed structure–function studies are required to fully elucidate the precise interactions of 25OHD with TRPV1 at the atomistic level.

With respect to the physiological relevance of these observations, TRPV1 activity is important in the activation of CD4^{+} T-cells (Bertin *et al.* 2014). Our results show that 25OHD and 1,25OHD significantly reduce the production of the cytokines TNFα and INFγ resulting from the T-cell receptor-mediated (TCR) activation of CD4^{+} T-cells. The involvement of TRPV1 in T-cell activation was confirmed in our cell system by the use of the TRPV1 antagonist capsazepine and by a previous study (Bertin *et al.* 2014). It is important to note that the expression of the vitamin D receptor in naïve T-cells is virtually absent (Von Essen *et al.* 2010). Thus, our results are consistent with 25OHD and 1,25OHD acting upon naïve T-cells via a VDR-independent mechanism, perhaps via suppression of TRPV1 activity. Precisely how this occurs remains to be elucidated experimentally. One

plausible explanation may involve interactions with the PKC-mediated potentiation of TRPV1, as we activated the CD4^{+} T-cells through co-stimulation of the TCR pathway using anti-CD3 and anti-CD28, which activate PKC (Rudd, 1996; Isakov & Altman, 2012). 25OHD may therefore reduce the PKC-mediated potentiation of TRPV1, subsequently reducing CD4^{+} T-cell cytokine production (Bertin *et al.* 2014). We also provide further evidence for a physiological role of this novel vitamin D–TRPV1 axis in nociception as 25OHD significantly decreases the capsaicin-induced calcium influx into trigeminal neurons, suggesting 25OHD may interact and compete with agonists to modulate and dampen nociceptive pain signalling pathways. Indeed, vitamin D deficiency has been linked to chronic pain (Holick, 2007; Helde-Frankling & Björkhem-Bergman, 2017). Of further interest is the fact that we observed this effect on TRPV1^{+} neurons within minutes of 25OHD application or removal, suggesting that the underlying mechanism is rapid and does not involve either TRPV1 trafficking or VDR-mediated gene transcriptional regulation, which would be expected to only occur on a longer time scale.

From a physiological perspective, we speculate that vitamin D may provide an elegant mechanism to induce basal TRPV1 activity that permits a small passive influx of calcium into the cell by virtue of the partial agonist effects of vitamin D being resistant to calcium-induced desensitization, thus regulating cellular function tonically. However, in the presence of a full endogenous agonist, vitamin D may act as an antagonist to reduce TRPV1-mediated calcium influx and excessive calcium-induced activation of a variety of cellular pathways in which TRPV1 is involved. Thus, the actions of vitamin D on TRPV1 activity, either alone or in concert with other endogenous TRPV1 ligands, may contribute to the diverse effects of vitamin D that have been widely reported in the literature.

It should be noted that the concentration of 100 nM 25OHD used in the majority of this study was chosen as it lies within the physiological circulating range observed in humans. Although a subject of some debate, the general consensus is that a circulating concentration of >70 nM 25OHD is considered normal, whereas vitamin D insufficiency occurs at levels of <70 nM 25OHD (Hollis, 2005; Holick, 2007). Therefore, it is highly plausible that the observed effects of vitamin D on TRPV1 activity play an important physiological role in many different biological systems in which vitamin D (or its deficiency) and TRPV1 have been previously characterized. Moreover, as circulating 1,25OHD levels are much lower (pM) than those of 25OHD, we speculate that any physiological effects of vitamin D on TRPV1 activity are mediated by 25OHD.

In summary, results from our study revealed the following key observations. (1) 25OHD is a partial TRPV1

agonist, whereby 25OHD is capable of weakly activating TRPV1 and antagonizing the stimulatory effects of the full TRPV1 agonists capsaicin and oleoyl dopamine. (2) 25OHD binds to TRPV1 within the same vanilloid binding pocket as capsaicin. (3) 25OHD inhibits the potentiating effects of PKC-mediated TRPV1 activity. (4) 25OHD reduces T-cell activation and trigeminal neuron calcium signalling mediated by TRPV1 activity. These results provide biophysical, molecular and cellular evidence that TRPV1 is a novel receptor for the biological actions of vitamin D in addition to the well-documented effects of vitamin D upon the nuclear VDR. Our results may have important implications for our current understanding of certain diseases in which TRPV1 activity and vitamin D deficiency have been implicated, such as chronic pain (Helde-Frankling & Björkhem-Bergman, 2017; Moran & Szallasi, 2018) and autoimmune diseases such as type 1 diabetes (Suri & Szallasi, 2008; Gregoriou *et al.* 2017; Murdaca *et al.* 2019). Further studies are therefore required to explore this intriguing possibility.

References

Altier C (2015). Spicing up the sensation of stretch: TRPV1 controls mechanosensitive piezo channels. *Sci Signal* **8**, fs3.

Altieri B, Muscogiuri G, Barrea L, Mathieu C, Vallone CV, Mascitelli L, Bizzaro G, Altieri VM, Tirabassi G, Balercia G, Savastano S, Bizzaro N, Ronchi CL, Colao A, Pontecorvi A & Della Casa S (2017). Does vitamin D play a role in autoimmune endocrine disorders? A proof of concept. *Rev Endocr Metab Disord* **18**, 335–346.

Barrea L, Savanelli MC, Di Somma C, Napolitano M, Megna M, Colao A & Savastano S (2017). Vitamin D and its role in psoriasis: An overview of the dermatologist and nutritionist. *Rev Endocr Metab Disord* **18**, 195–205.

Bassi MS, Gentile A, Iezzi E, Zagaglia S, Musella A, Simonelli I, Gilio L, Furlan R, Finardi A, Marfia GA, Guadalupi L, Bullitta S, Mandolesi G, Centonze D & Buttari F (2019). Transient receptor potential vanilloid 1 modulates central inflammation in multiple sclerosis. *Front Neurol* **10**, 30.

Benham CD, Gunthorpe MJ & Davis JB (2003). TRPV channels as temperature sensors. *Cell Calcium* **33**, 479–487.

Berezowska M, Coe S & Dawes H (2019). Effectiveness of vitamin D supplementation in the management of multiple sclerosis: a systematic review. *Int J Mol Sci* **20**, 1301.

Bertin S, Aoki-Nonaka Y, de Jong PR *et al.* (2014). The ion channel TRPV1 regulates the activation and proinflammatory properties of CD4^{+} T cells. *Nat Immunol* **15**, 1055–1063.

Bhave G, Hu HJ, Glauner KS, Zhu W, Wang H, Brasier DJ, Oxford GS & Gereau IV RW (2003). Protein kinase C phosphorylation sensitizes but does not activate the capsaicin receptor transient receptor potential vanilloid 1 (TRPV1). *Proc Natl Acad Sci U S A* **100**, 12480–12485.

Blumberg PM, Pearce LV & Lee J (2011). TRPV1 activation is not an all-or-none event: TRPV1 partial agonism/antagonism and its regulatory modulation. *Curr Top Med Chem* **11**, 2151–2158.

Cantorna M, Snyder L, Lin Y-D & Yang L (2015). Vitamin D and 1,25(OH)2D regulation of T cells. *Nutrients* **7**, 3011–3021.

Carnevale V & Rohacs T (2016). TRPV1: A target for rational drug design. *Pharmaceuticals* **9**, 52.

Caterina MJ, Schumacher MA, Tominaga M, Rosen TA, Levine JD & Julius D (1997). The capsaicin receptor: A heat-activated ion channel in the pain pathway. *Nature* **389**, 816–824.

Christie S, Wittert GA, Li H & Page AJ (2018). Involvement of TRPV1 channels in energy homeostasis. *Front Endocrinol* **9**, 420.

Chu CJ, Huang SM, De Petrocellis L, Bisogno T, Ewing SA, Miller JD, Zipkin RE, Daddario N, Appendino G, Di Marzo V & Walker JM (2003). *N*-oleoyldopamine, a novel endogenous capsaicin-like lipid that produces hyperalgesia. *J Biol Chem* **278**, 13633–13639.

Elokely K, Velisetty P, Delemotte L, Palovcak E, Klein ML, Rohacs T & Carnevale V (2016). Understanding TRPV1 activation by ligands: Insights from the binding modes of capsaicin and resiniferatoxin. *Proc Natl Acad Sci U S A* **113**, E137–E145.

Gram DX, Holst JJ & Szallasi A (2017). TRPV1: A potential therapeutic target in type 2 diabetes and comorbidities? *Trends Mol Med* **23**, 1002–1013.

Grammatiki M, Rapti E, Karras S, Ajjan RA & Kotsa K (2017). Vitamin D and diabetes mellitus: Causal or casual association? *Rev Endocr Metab Disord* **18**, 227–241.

Green DP, Ruparel S, Roman L, Henry MA & Hargreaves KM (2013). Role of endogenous TRPV1 agonists in a postburn pain model of partial-thickness injury. *Pain* **154**, 2512–2520.

Gregoriou E, Mamais I, Tzanetakou I, Lavranos G & Chrysostomou S (2017). The effects of vitamin D supplementation in newly diagnosed type 1 diabetes patients: systematic review of randomized controlled trials. *Rev Diabet Stud* **14**, 260–268.

Helde-Frankling M & Björkhem-Bergman L (2017). Vitamin D in pain management. *Int J Mol Sci* **18**, 2170.

Holick MF (2007). Vitamin D deficiency. *N Engl J Med* **357**, 266–281.

Hollis BW (2005). Circulating 25-hydroxyvitamin D levels indicative of vitamin D sufficiency: implications for establishing a new effective dietary intake recommendation for vitamin D. *J Nutr* **135**, 317–322.

Isakov N & Altman A (2012). PKC-theta-mediated signal delivery from the TCR/CD28 surface receptors. *Front Immunol* **3**, 273.

Julius D (2013). TRP channels and pain. *Annu Rev Cell Dev Biol* **29**, 355–384.

Kato S (2000). The function of vitamin D receptor in vitamin D action. *J Biochem* **127**, 717–722.

Lee L-Y & Gu Q (2009). Role of TRPV1 in inflammation-induced airway hypersensitivity. *Curr Opin Pharmacol* **9**, 243–249.

Li X, Liu Y, Zheng Y, Wang P & Zhang Y (2018). The effect of vitamin D supplementation on glycemic control in type 2 diabetes patients: a systematic review and meta-analysis. *Nutrients* **10**, 375.

Liao M, Cao E, Julius D & Cheng Y (2013). Structure of the TRPV1 ion channel determined by electron cryo-microscopy. *Nature* **504**, 107–112.

Lukacs V, Thyagarajan B, Varnai P, Balla A, Balla T & Rohacs T (2007). Dual regulation of TRPV1 by phosphoinositides. *J Neurosci* **27**, 7070–7080.

Mandadi S, Numazaki M, Tominaga M, Bhat MB, Armati PJ & Roufogalis BD (2004). Activation of protein kinase C reverses capsaicin-induced calcium-dependent desensitization of TRPV 1 ion channels. *Cell Calcium* **35**, 471–478.

McLaughlin L, Clarke L, Khalilidehkordi E, Butzkueven H, Taylor B & Broadley SA (2018). Vitamin D for the treatment of multiple sclerosis: a meta-analysis. *J Neurol* **265**, 2893–2905.

Moran MM (2018). TRP channels as potential drug targets. *Annu Rev Pharmacol Toxicol* **58**, 309–330.

Moran MM & Szallasi A (2018). Targeting nociceptive transient receptor potential channels to treat chronic pain: current state of the field. *Br J Pharmacol* **175**, 2185–2203.

Movahed P, Jönsson BAG, Birnir B, Wingstrand JA, Jørgensen TD, Ermund A, Sterner O, Zygmunt PM & Högestätt ED (2005). Endogenous unsaturated C18 N-acylethanolamines are vanilloid receptor (TRPV1) agonists. *J Biol Chem* **280**, 38496–38504.

Murdaca G, Tonacci A, Negrini S, Greco M, Borro M, Puppo F & Gangemi S (2019). Emerging role of vitamin D in autoimmune diseases: An update on evidence and therapeutic implications. *Autoimmun Rev* **18**, 102350.

Nersesyan Y, Demirkhanyan L, Cabezas-Bratesco D, Oakes V, Kusuda R, Dawson T, Sun X, Cao C, Cohen AM, Chelluboina B, Veeravalli KK, Zimmermann K, Domene C, Brauchi S & Zakharian E (2017). Oxytocin modulates nociception as an agonist of pain-sensing TRPV1. *Cell Reports* **21**, 1681–1691.

Numazaki M, Tominaga T, Toyooka H & Tominaga M (2002). Direct phosphorylation of capsaicin receptor VR1 by protein kinase Cε and identification of two target serine residues. *J Biol Chem* **277**, 13375–13378.

Omari SA, Adams MJ & Geraghty DP (2017). TRPV1 channels in immune cells and hematological malignancies. *Adv Pharmacol* **79**, 173–198.

Pike JW & Meyer MB (2010). The vitamin D receptor: new paradigms for the regulation of gene expression by 1,25-dihydroxyvitamin D3. *Endocrinol Metab Clin North Am* **39**, 255–269.

Prescott ED & Julius D (2003). A modular PIP2 binding site as a determinant of capsaicin receptor sensitivity. *Science* **300**, 1284–1288.

Ross RA (2003). Anandamide and vanilloid TRPV1 receptors. *Br J Pharmacol* **140**, 790–801.

Rudd CE (1996). Upstream-downstream: CD28 cosignaling pathways and T cell function. *Immunity* **4**, 527–534.

Ryu S, Liu B, Yao J, Fu Q & Qin F (2007). Uncoupling proton activation of vanilloid receptor TRPV1. *J Neurosci* **27**, 12797–12807.

Spicarova D & Palecek J (2009). The role of the TRPV1 endogenous agonist *N*-oleoyldopamine in modulation of nociceptive signaling at the spinal cord level. *J Neurophysiol* **102**, 234–243.

Studer M & McNaughton PA (2010). Modulation of single-channel properties of TRPV1 by phosphorylation. *J Physiol* **588**, 3743–3756.

Suri A & Szallasi A (2008). The emerging role of TRPV1 in diabetes and obesity. *Trends Pharmacol Sci* **29**, 29–36.

Szallasi A, Cortright DN, Blum CA & Eid SR (2007). The vanilloid receptor TRPV1: 10 years from channel cloning to antagonist proof-of-concept. *Nat Rev Drug Discov* **6**, 357–372.

Trott O & Olson A (2010). Autodock vina: improving the speed and accuracy of docking. *J Comput Chem* **31**, 455–461.

Tsui H, Razavi R, Chan Y, Yantha J & Dosch HM (2007). "Sensing" autoimmunity in type 1 diabetes. *Trends Mol Med* **13**, 405–413.

Von Essen MR, Kongsbak M, Schjerling P, Olgaard K, Ødum N & Geisler C (2010). Vitamin D controls T cell antigen receptor signaling and activation of human T cells. *Nat Immunol* **11**, 344–349.

Wallace AC, Laskowski RA & Thornton JM (1995). Ligplot: A program to generate schematic diagrams of protein-ligand interactions. *Protein Eng Des Sel* **8**, 127–134.

Wang S, Joseph J, Ro JY & Chung MK (2015). Modality-specific mechanisms of protein kinase C-induced hypersensitivity of TRPV1: S800 is a polymodal sensitization site. *Pain* **156**, 931–941.

Wang S, Yamamoto S, Kogure Y, Zhang W, Noguchi K & Dai Y (2016). Partial activation and inhibition of TRPV1 channels by evodiamine and rutaecarpine, two major components of the fruits of *Evodia rutaecarpa*. *J Nat Prod* **79**, 1225–1230.

Yang F, Xiao X, Cheng W, Yang W, Yu P, Song Z, Yarov-Yarovoy V & Zheng J (2015). Structural mechanism underlying capsaicin binding and activation of the TRPV1 ion channel. *Nat Chem Biol* **11**, 518–524.

Yang J & Zhang Y (2015). I-TASSER server: New development for protein structure and function predictions. *Nucleic Acids Res* **43**, W174–W181.

Yong WC, Sanguankeo A & Upala S (2017). Effect of vitamin D supplementation in chronic widespread pain: a systematic review and meta-analysis. *Clin Rheumatol* **36**, 2825–2833.

Yu Y, Carter CRJ, Youssef N, Dyck JRB & Light PE (2014). Intracellular long-chain acyl CoAs activate TRPV1 channels. *PLoS One* **9**, e96597.

Zhong B & Wang DH (2008). *N*-oleoyldopamine, a novel endogenous capsaicin-like lipid, protects the heart against ischemia-reperfusion injury via activation of TRPV1. *Am J Physiol Heart Circ Physiol* **295**, H728–H735.

Additional information

Competing interests

The authors declare no competing interests.

Author contributions

TRPV1 calcium imaging studies, analysed data and revised the manuscript. R.P. performed the TRPV1 modelling and docking studies and analysed the data. K.P. contributed to the design of the calcium imaging studies, analysed data, and revised the manuscript. Y.Y. conducted some of the electrophysiology experiments and analysed data. R.K. conducted the CD4+ T-cell flow cytometry studies and analysed data. B.B. performed the trigeminal neuron calcium imaging studies and analysed data. A.B. provided major technical support and manuscript revision. D.G. provided technical support, theoretical input and analysed data for the CD4+ T-cell flow cytometry studies. S.A.C. performed part of the TRPV1 modelling and docking studies. K.O. and M.H. provided cell culture and transfection expertise and revised the manuscript. T.B. designed the flow cytometry experiments and revised the manuscript. M.J.L. designed and supervised the TRPV1 structural modelling and docking studies and revised the manuscript. P.E.L. conceived the hypothesis, helped design the experiments, generated the final figures and revised the manuscript. All authors have read and approved the final version of this manuscript and agree to be accountable for all aspects of the work in ensuring that questions related to the accuracy or integrity of any part of the work are appropriately investigated and resolved. All persons designated as authors qualify for authorship, and all those who qualify for authorship are listed.

Supporting information

Additional supporting information may be found online in the Supporting Information section at the end of the article.

Statistical Summary Document.